BEHAVIOR OF HIGHLY POROUS CHARS DURING OXIDATION IN REGIME I

Ezra Bar-Ziv
Department of Mechanical Engineering, Ben-Gurion University of the Negev, and
Nuclear Research Center - Negev, P.O. Box 9001
Beer-Sheva, Israel

Keywords: Coal Char, Pore Structure, Char Oxidation

INTRODUCTION

The pore structure and its evolution during burnout are major influence on the mechanism of conversion of highly porous chars. Recently, this topic has been presented in several studies [1-8]. Pore structure, can be studied from macroscopic quantities that can be presently measured routinely. Evolution of the pore structure and its influence on char reactivity can be studied from changes in (1) external dimensions, (2) physical properties, and (3) reaction rate. In this review we concentrate on the role of pore structure for char reactivity and narrowed down to highly porous chars with no volatile or mineral matters. We present an overview, that includes only experimental results, on processes and properties for single particles of highly porous synthetic chars oxidized by oxygen. We will show that there is a general behavior connected to the evolution of the pore structure.

Spherocarb particles (synthetic char) were chosen as a model material because they have relatively well defined and reproducible, are quite spherical and have very close pore structure to certain coal chars. Only results from kinetically controlled conditions (regime I) are included. The particles were with initial total porosities in the range 70-80%, with diameters in the range 150-250 μm, oxidized in air or in pure oxygen, with or without moisture, in the temperature range 700-1200 K. Care was taken to include results that obey the Thiele criterion. Four topics will be discussed: (1) Changes in external shape of particles. (2) Fragmentation. (3) Changes in physical properties. (4) Oxidation rate.

Most of the results presented here were obtained with an electrodynamic chamber (EDC). For details on the EDC see for example in Refs. [5,9-17]. The EDC has been developed and applied for kinetic studies of single particles at high temperatures in many studies. The main advantages of the EDC are: (1) Ability to study the kinetics of a single particle in well controlled conditions. (2) Ability to characterize the particle prior to reaction and monitor the important quantities in real time during reaction. (3) The elimination of heat and mass transfer limitations existing in other methods that restrict kinetic measurements to slow rates. (4) The ability to study particle to particle variations. The quantities that were measured for single particles are: weight, shape and dimensions, density and porosity, temperature, total surface area, thermal conductivity, heat capacity, reaction rate.

OBSERVATIONS AND DISCUSSION

1. Changes in External Shape

Decrease in external dimensions of a particle is referred to as shrinkage. If reaction occurred in external surface, as in regime III and partially in regime II, change in external dimensions are understandable and expected. However, in regime I where oxygen is available to all active sites, the changes in the external dimensions must reflect the changes in the internal morphology. Two types of shrinkage have been observed: uniform and non-uniform shrinkage.

Uniform Shrinkage. Shrinkage has been observed in various studies [15,16,18-20] for highly porous synthetic chars oxidized in regime I. It has been shown [21] that shrinkage is a general phenomenon occurring for a variety of carbonaceous materials at ranges varying from tens of nanometers [22] to 70 mm [23]. Shrinkage factor was defined as the ratio of volume to initial volume. Figure 1 shows results for the shrinkage factor vs. conversion. The results were gathered from about forty different experiments covering the ranges of diameters, temperatures, and densities mentioned above. The shrinkage factor decreases monotonically with conversion not obeying neither the shrinking sphere model (linear decrease, constant density) nor the hollow sphere model (constant diameter). It was established [19] that shrinkage is not due to external surface reaction, but is a homogeneous reaction-induced densification of the microporous solid phase. Shrinkage is ascribed to rearrangement in the microstructure. Thus, if shrinkage is a result of morphological changes, other properties connected to the pore structure must change accordingly. Porosity (or density) and internal surface area were extensively investigated. Figure 2 presents results for normalized density vs. conversion. Density decreases with conversion to approximately half its initial value at about 85% conversion. Although at high conversion the results are scattered a clear indication of increase in density is seen. This increase may be due to densification of the solid, which is also reflected in the thermal conductivity as will be shown below. The total surface area results are less dramatic, but display the same behavior.

Non-Uniform Shrinkage. Non-uniform shrinkage has been observed [15,17] when a particle was irradiated non-uniformly. It has been quantitatively investigated in a systematic manner [24]. Results

of the shrinkage factor for non-uniform shrinkage from many runs show a similar trend to that seen in Fig. 2, however, with some meaningful differences. The shrinkage factor is equal in the two cases from zero conversion to about 50% conversion, then there is a systematic deviation between the two phenomena. Clearly, the deviation is due to different propagation of the pore structure in the two cases. The important finding is that non-uniform shrinkage is also a general phenomenon that is independent on initial values of porosity and diameter, and reaction rate. The major conclusion from both uniform and non-uniform shrinkage is that the pore structure as represented by shape, external dimension, porosity and total surface area, is undergoing a pattern that is equal to all cases regardless the initial conditions or reaction rates.

2. Fragmentation

Fragmentation is another phenomenon that can shed light on the nature of the pore structure and its evolution. The mechanism that arises from the evolution of the pore structure is usually referred to as percolation fragmentation for oxygen percolates through the porous structure and "erodes" the carbon microcrystals with a possible subsequent fragmentation. Percolation fragmentation of carbon spheres during oxidation was reported in a number of studies [25-28]. A theory for percolation fragmentation was developed and showed that for any homogeneous material, fragmentation will occur at a critical porosity of about 70% [28]. Recent observation [15,24] showed also local percolation fragmentation. These results strengthen the thesis that fragmentation is a threshold phenomenon that occurs above a critical porosity, as predicted in [28]. More than one hundred experiments were carried out up to 80% conversion. None of these showed any fragmentation but a few (two or three) showed formation of a hole in the center of the particle. This was indicative to local percolation fragmentation and was predicted by a recent model [23]. Another twenty-two experiments were conducted up to completion and half of them developed holes in the particle center. Out of these, only a few particles broke into two particles. The formation of holes is resulting from the evolution of the pore structure. In all experiments the particle underwent non-uniform shrinkage, transforming the initially spherical particle into a disk at 50-60% conversion. At higher conversion (above 85%) about half of the particles developed holes in the center. Figure 3 presents a typical conversion vs. time curve with a sequence of shadowgraphs depicting the shape development of a Spherocarb particle of 204 micron diameter at various conversions, oxidized in air at T=920 K. Spatial dimensions of the particle are included in the figure. Three regions of oxidation are observed: (i) at low conversion the particle hardly loses mass; (ii) quick mass loss from about 4% conversion to about 95 conversion; and (iii) very slow mass loss from about 95% up to completion. The initially spherical particle turned into a disk at about 60% conversion.

To conclude, formation of holes is a manifestation of the pore structure evolution displayed more pronouncely in disk-shaped particles, formed due to non-uniform shrinkage. Finally, breaking of the particle is a mere coincidence and a random incident where a particle can break due to growth and overlap of large macropores. The important thing is that in all these experiments, the behavior during oxidation was identical for all particles, regardless of initial conditions and oxidation rate.

3. Changes in Physical Properties

Some physical properties of chars depend on distribution of voids and solid microcrystals. Other properties are the reflection of the details of the pore structure, such as connectivities, microcrystal dimensions. Density, total surface area, and heat capacity, belong to the former and thermal conductivity to the latter. In both groups the behavior of the properties depend on the evolution of the pore structure. Thermal conductivity was systematically studied recently [16,29,30] and was shown to be a very strong tool for details of the pore structure and its evolution.

Thermal conductivity. It has been clearly shown [29] that all previous concepts for highly porous materials cannot explain the strong observed change in thermal conductivity with conversion. The surprising result is that total porosity plays a minor role in the evolution of the thermal conductivity. A model showing that thermal conductivity is a property that is highly capacious of the information on the internal microstructure has been developed [29]. Main conclusions are that thermal conductivity is affected by: (1) Consumption of carbon on the internal surface. (2) Coalescence of microcrystals. (3) Activation of intercrystal joints. The change in thermal conductivity k_p with conversion was found to be similar for all particles, regardless of initial conditions or reaction rate. Figure 4 shows k_p/k_{min} (min refer to minimum) for eleven particles at different temperatures. The value of k_p/k_{min} decreases with conversion by a factor of 5-7 from zero to 30% conversion. k_p/k_{min} remains constant until 80% conversion, then it rises by a factor of 2-3 from about 90% conversion to final burnout. The results from the common models [32] show a very poor match to the experimental data. k_p/k_{min} decreases much slower with conversion at low conversions than observed and it behaves opposite to the observed behavior at high conversions. However, a good fit to the model that includes the features of the micromedium was obtained. The significance of these results is that it is most probable that the main role in the change in thermal conductivity, both at low and high conversion, is the change in the dimensions of microcrystal joints. At low conversion the fast

decrease in k_p can be explained by activation of intercrystal joints, i.e., breaking the joints. The increase of thermal conductivity at high conversion can be ascribed to the increase in the radius of an intercrystal joint. The increase of a joint is a manifestation of better ordering of an individual microcrystal. The abruptness of the increase is likely to reflect the spontaneity of the process. Therefore, we interpret the increase in k_p as an indication of conversion induced graphitization. An indication to graphitization at final burnout stages can be found in a recent study [31] where high-resolution tunneling electron microscopy was used. We should, therefore, conclude that the more likely model to represent thermal conductivity is the one that considers the details of the micromedium structure (including nature of connections between microcrystals) and does not consider the porous structure as a mere two-phase medium -- solid/gas -- as represented in most thermal conductivity models [32]. This conclusion strengthens the importance of thermal conductivity for the understanding of changes in the pore structure of highly porous media in general, and for chars in particular.

4. Mass Transients

Numerous measurements of mass loss were carried out for Spherocarb particles reacting in regime I at the range of conditions specified above. A convenient way of presenting the data is conversion vs. normalized time (by time at half conversion -- $t_{1/2}$), as shown in Fig. 5. The various results fall within one curve, within experimental uncertainty (larger scatter at long time region). Three regions of behavior are observed: (1) slow mass loss with time in the early stages of burnout; (2) fast reaction; and (3) slow reaction at final burnout. Figure 6 shows normalized reaction rate (with $t_{1/2}$) vs. conversion measured from different studies at various temperatures. The fact that all results (transients and rates) can be normalized by one quantity ($t_{1/2}$) has a very strong significance: All three stages of conversion are strongly related to the same mechanism. Note that this mechanism prevails for all conditions of regime I. One can deduce that consumption of carbon is governed by one mechanism. Dividing the consumption process into two stages, one at which reaction sites are activated and the other is the actual gasification (solid carbon turns into gaseous carbon, i.e., CO or CO_2). Clearly, from the results of Figs. 5 and 6, gasification (stage 2) cannot be the rate determining step for it is unlikely that the two mechanisms have the same activation energies. Thus, the only conclusion that one can draw from this behavior is that activation of sites is the dominant mechanism that governs the consumption of carbon. Active sites, however, are a direct consequence of the evolution of the pore structure. Therefore, the reactivity of chars as physical properties discussed above are also a direct consequence of the pore structure.

In light of this conclusion one can draw a picture of the reactivity behavior of highly porous chars. In the early stages of burnout reactive sites are very scarce and reaction is very slow. As reaction proceeds, morphology and crystallinity change, and as a consequence reactive sites start to build up and reactivity increases. At some stage, reaction progressed such that reactive sites start to decline, resulting in decreasing of reaction rate, that occurs at high conversion. In fact from this description one can deduce that the behavior of reaction rate is a consequence of the change in active sites an that the intrinsic reaction rate is constant with conversion.

SUMMARY

The selection of Spherocarb particles has given us the opportunity to examine physicochemical processes under well defined and reproducible conditions. Differences were only on total porosity and diameter. The numerous results obtained in a wide range of conditions has provided a wide-angled view that can help elucidate the governing mechanisms for oxidation. Each of the physical properties studied has behaved in a certain quantitative way equal in all experiments. Similarly, the phenomena of shrinkage and fragmentation showed, each, clear and reproducible pathways. Dependence of reaction rate on temperature, on oxygen concentration, on conversion, on time has shown also a clear pattern regardless of initial conditions. From these observations it is inevitable to reach the conclusion that all these processes and quantities are related to the pore structure and its fine tunes. The most striking evidence is the results of conversion versus normalized time that showed clearly that all stages of conversion must be all connected to one mechanism. This conclusion, however, is only circumstantial. We do not have yet results from direct observation of microscopic changes (morphology and crystallinity) for Spherocarb particles. Still the numerous macroscopic data can serve as strong indication of the microscopic processes. Insights can be gained if a model that includes the microscopic features and can reconstruct the numerous physicochemical experimental data, by minimum parameter fitting.

References

1. Sahimi, A., Gavalas, G.R., and Tsotsis, T.T., Chem. Eng. Sci. **45**:1443 (1990).
2. Hurt, R.H., Sarofim, A.F., and Longwell, J.P., Energy & Fuel **5**:290 (1991).
3. Miccio, F., and Salatino, P., 24th Sym. (Int.) on Combustion, The Combustion Institute, Pittsburgh, 1992, pp. 1145-1151.
4. Salatino, P., Miccio, F., and Massimilla, L., Combust. Flame **95**:342 (1993).
5. D'Amore, M.D., Tognotti, L., Sarofim, A.F., Combust. Flame, **95**:374 (1993).
6. Salatino, P., Miccio, F., 24th Sym. (Int) on Combustion, The Combustion Institute, Pittsburgh, PA, 1994, pp. 1145-1151.
7. Kantorovich, I.I, and Bar-Ziv, E., Combust. Flame **97**:61 (1994).
8. Kantorovich, I.I, and Bar-Ziv, E., Combust. Flame **97**:79 (1994).
9. D'Amore, M., Dudek. R.D., Sarofim, A.F., and Longwell, J.P., Powder Technology **56**:129 (1988).
10. Dudek, D.R., Fletcher, T.H., Longwell, J.P., and Sarofim, A.F., Int. J. Heat Mass Transfer **31**:863 (1988).
11. Bar-Ziv, E., Jones, D.B., Spjut, R.E., Dudek, D.R., Sarofim, A.F., and Longwell, J.P., Combustion and Flame **75**: 81 (1989).
12. Tognotti, L., Longwell, J.P., and Sarofim, A.F., 23rd Sym. (Int.) on Combustion, The Combustion Institute, Pittsburgh, 1990, pp. 1207-1213.
13. Bar-Ziv, E., Longwell, J.P., Sarofim, A.F., Energy and Fuels **5**:227 (1991).
14. Bar-Ziv, E., and Sarofim, A.F., Prog. Energy Comb. Sci. **17**:10 (1991).
15. Weiss, Y., and Bar-Ziv, E., Combust. Flame **95**:362 (1993).
16. Weiss, Y., Ben-Ari, Y., Kantorovich, I.I., Bar-Ziv, E., Krammer, G., Modestino, A., and Sarofim, A.F., 25th Sym. (Int.) on Combustion, The Combustion Institute, Pittsburgh, PA 1994, pp. 519-525.
17. Weiss, Y., and Bar-Ziv, E., Combustion and Flame **101**:452 (1995).
18. Weiss, Y., Ph.D. Thesis, Ben-Gurion University of the Negev, 1995.
19. Hurt, R.H., Dudek, D.R., Longwell, J.P., and Sarofim, A.F., Carbon **25**:433 (1988).
20. Dudek, D.R., Ph.D. Thesis, Massachusetts Institute of Technology, Cambridge, MA, 1988.
21. Hurt, R.H., Sarofim, A.F., and Longwell, J.P., Combust. Flame **95**:430 (1993).
22. Ishiguro, T., Suzuki, N., Fujitani, Y., and Morimoto, H., Combust. Flame **85**:1 (1991).
23. Easler, T.E., Bradt, R.C., and Walker, P.L., Fuel **69**:124 (1990).
24. Zhang, X., Dukhan, A., Kantorovich, I.I., and Bar-Ziv, E., "Bulk Fragmentation of Highly Porous Char Particles in Regime I," Combust. Flame **XX**:XXX (1995).
25. Davis, H., and Hottel, H.C., Ind. Eng. Chem. **26**:889 (1934).
26. Walker, P.L., Jr., Rusino, F., and Austin, L.G., Adv. Catal. **11**:133 (1957).
27. Dutta, S., Wen, C.Y., and Belt, R.J., Ind. Eng. Chem. Proc. Des. Dev. **16**:20 (1977).
28. Kerstein, A.R., and Niksa, S., 20th Sym. (Int.) on Combustion, The Combustion Institute, Pittsburgh, 1984, pp. 941-949.
29. Kantorovich, I.I, and Bar-Ziv, E., "The Effect of Microstructural Transformation on the Evolution of Thermal Conductivity of Highly Porous Chars during Oxidation," Combust. Flame, (1995).
30. Dukhan, A., Zhang, X., Kantorovich, I.I., and Bar-Ziv, E., "Thermal Conductivity and Porosity of Char Particles in Regime I," submitted to 26th Sym. (Int.) on Combustion, The Combustion Institute, Pittsburgh, PA 1996.
31. Davis, K.A., Hurt, R.H., Yang, N.Y.C., nd Headly, T.H., 25th Sym. (Int.) on Combustion, (The Combustion Institute, Pittsburgh, PA 1994), pp. XXX-XXX.
32. Hashin, Z. and Shtrinkman, S., J. Appl. Phys. **10**:3125 (1962).

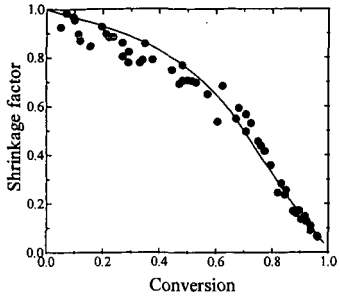

Figure 1. Shrinkage factor versus conversion for uniform shrinkage [9,16,19,20].

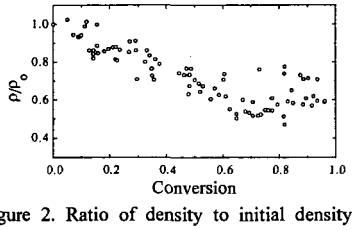

Figure 2. Ratio of density to initial density vesrus conversion [7,17,19,20].

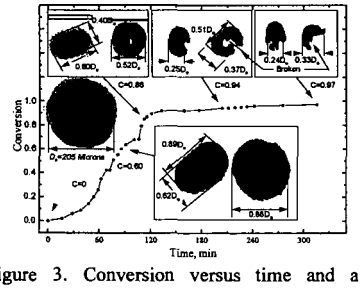

Figure 3. Conversion versus time and a sequence of shadowgraphs presenting the development of shape of a 204 microns Spherocarb particle vs. conversion oxidized in air at 920 K; C is conversion, l is length, and w is width.

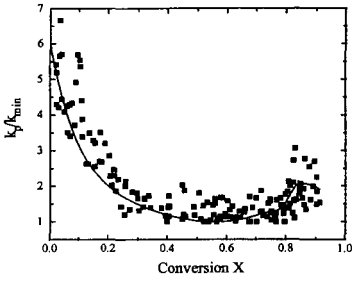

Figure 4. Ratio of thermal conductivity to its minimum value, k_p/k_{min} as a function of conversion.

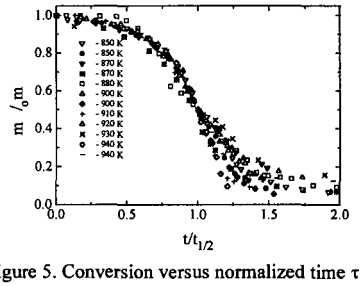

Figure 5. Conversion versus normalized time τ (by time at half conversion -- $t_{1/2}$) for particles oxidized under un-even temperature field.

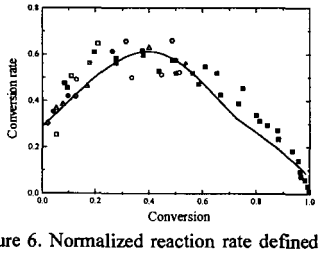

Figure 6. Normalized reaction rate defined as dC/dτ versus conversion [9,12,20].